Numerical Modeling and Measurement of Apis Mellifera Radar Scattering Properties

Omar Alzaabi, *Member, IEEE*, Mohammad M. Al-Khaldi, *Member, IEEE*, Kenneth Ayotte, Diego Peñaloza, Julio Urbina, *Member, IEEE*, James K. Breakall, *Senior Member, IEEE*, Michael Lanagan, *Member, IEEE*, Harland M. Patch, and Christina M. Grozinger

***Abstract*— This study investigates a means through which commercially available computational electromagnetic modeling software can be used to predict radar cross sections (RCSs) of airborne organisms of interest as a preliminary step toward enabling detection and tracking of these organisms. This work aims to analyze this framework for the specialized case of the honey bee (*Apis mellifera*), given its critical role in food security as a major pollinator of agricultural crops. A Method-of-Moment (MoM) solver made available by Altair's FEKO is used to conduct the analysis over varying frequencies, illumination angles, and polarizations. A high degree of correlation between measured and modeled cross sections is noted. Maximum RCS root-mean-square errors (RMSEs) between the two are approximately 4 and 5 dB relative to 1 m^2 (dBsm) for Horizontal polarization (H-pol) and Vertical polarization (V-pol) X-band measurements, respectively. Findings of this study also highlight the sensitivity of both modeled and measured RCS estimates to the dielectric properties of honey bees and the corrupting effects that this may have if not accounted for accurately, where errors are shown to increase from 2 to 5 dBsm, but without significantly corrupting the overall RCS azimuth profile.**

***Index Terms*— Dielectric characterization, FEKO, method of moments, radar cross section (RCS).**

I. Introduction

AIRBORNE insects play a major role in a vast array of ecological processes, including nutrient cycling, biotic interactions, pollination, and population dynamics, to name a few [1]–[4]. Honey bees (*Apis mellifera*) are particularly important since they serve as a major pollinator of agricultural crops. Nearly, 90% of flowering plant species and almost 75% of major global agricultural crops benefit from honey bees and other pollinators moving their pollen among flowers, which is critical for seed and fruit set. In addition to the economic impact of pollinated crops, these crops provide critical nutrients for human diets. However, beekeepers report high annual losses of managed honey bee colonies every year, with annual losses in the United States averaging at approximately 40% [5]. Mitigating these losses requires a detailed understanding of honey bee flight behavior, so researchers can better model how and where bees forage for food and where they may be exposed to pesticides [6].

Several schemes exist to analyze airborne insect behavior and migratory tendencies, including transponder fitting, mark–recapture techniques, genetic analysis, pollen mapping, nest–forager association, nest–plant association, and nest site addition [7]. While these techniques provide some pertinent information into bee behavior and habits, their practical efficacy provides limited insights due to the large footprint (≈10 km from their colony [8]) typically covered and the need for precise [8] alignments in the case of transponder fitting [9].

Recent studies [10]–[12] have proposed the use of radar-based characterization for the tracking of airborne animals and insects of interest. A similar study is undertaken here with a particular emphasis on the use of this methodology in the context of honey bees. Emphasis is also placed on the impact of accurate knowledge of the target's dielectric properties and on the ability to model its radar cross section (RCS). Measures of RCS are dependent on a number of characteristics, including size, shape, material, and aspect of the target, as well as the wavelength and polarization of the transmitted radiation with respect to the orientation of the target. Therefore, modeling is used to account for the bulk of the aforementioned dependencies, and these models are subsequently confirmed with an experimental characterization of insect RCS over a wide range of frequencies, illumination angles, and polarizations. This goes to enable future efforts in radar-based tracking and detection of honey bees. The completely passive nature of this approach promises superior performance compared to some of the aforementioned schemes as they require no physical fixtures, fitting, or manipulation of bees through the addition and application of extra harnesses or chemical exposure to bee populations.

Next, Section II outlines the theoretical basis and experimental studies undertaken to characterize average honey bee dielectric properties through scattering parameter

Manuscript received October 11, 2020; revised November 13, 2020; accepted December 28, 2020. Date of publication February 2, 2021; date of current version December 17, 2021. *(Corresponding author: Omar Alzaabi.)*

Omar Alzaabi is with the Department of Electrical Engineering and Computer Science, Khalifa University, Abu Dhabi 127788, UAE (e-mail: oalzaabi@ieee.org).

Mohammad M. Al-Khaldi and Kenneth Ayotte are with the Department of Electrical and Computer Engineering and ElectroScience Laboratory, The Ohio State University, Columbus, OH 43210 USA.

Diego Peñaloza, Julio Urbina, and James K. Breakall are with the Department of Electrical Engineering, Pennsylvania State University, University Park, PA 16802 USA.

Michael Lanagan are with the Department of Engineering Science and Mechanics, Pennsylvania State University, University Park, PA 16802 USA.

Harland M. Patch and Christina M. Grozinger are with the Department of Entomology, Pennsylvania State University, University Park, PA 16802 USA.

Digital Object Identifier 10.1109/LGRS.2020.3048654

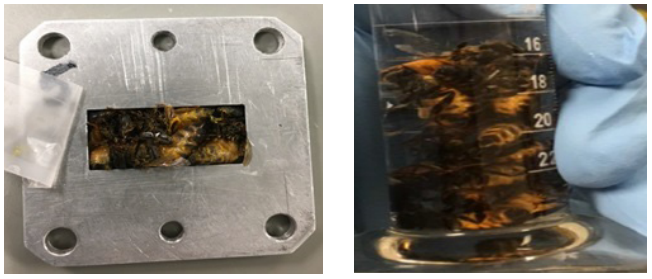

(a) (b)

Fig. 1. (a) Depiction of fabricated measurement waveguide filled with honey bees. (b) Illustration of acetone-based volumetric displacement approach for determining "bees-only" permittivity using Landau & Lifshitz and Looyenga dielectric mixing models.

waveguide-based measurements. Section III provides an overview of the experimental setup and analysis used to validate modeled RCS signatures obtained using FEKO [13] and outlines relevant experimental considerations. Section IV provides an analysis of results and identifies practical considerations, which influenced measured RCS profiles relative to those modeled. Section VI provides conclusions of this study and recommendations for future work.

II. Dielectric Characterization of Test Samples

Dielectric properties of the honey bee body form an integral part of the honey bee RCS. To develop an estimate of the dielectric properties of the honey bee targets, a systematic approach is adopted in which the scattering parameters (S-parameters), describing wave propagation under matched loads, for a honey bee filled waveguide are used to derive an ensemble average of the bee's dielectric properties.

A. Experimental Setup and Considerations

Practical considerations dictate the choice of frequency range across which an average measure of the honey bee's dielectric properties is obtained. This includes the fact that, for low frequencies, the dimensions of the waveguide will be large, which, in turn, requires the packing of a large number of bees. For higher frequencies, waveguide cutoff increases, and the size of the aperture is reduced significantly, thereby not allowing for the addition and packing of the waveguide with honey bee samples. It is, therefore, determined that measurements made at the X-band between a frequency range of 8–12 GHz provide a representative measure of the *Apis millifera* dielectric properties while circumventing some of the aforementioned practical limitations. The *Apis mellifera* samples are packed into a rectangular waveguide obtained by machining waveguide flange stock depicted in Fig. 1 to a thickness of 3 mm with aperture height (h) and width (w) at 1.27 and 2.29 cm, respectively, thereby allowing for a frequency of operation range $\approx 8.2 \leq f \leq 12.4$ GHz.

B. Computing Average Permittivity

Well-established properties [14] are used to derive the relationship between the complex scattering parameters S_{11} and S_{21} and the average dielectric properties of the *Apis mellifera* honey bees. The scattering parameters are intrinsically dependent on the waveguide's filling materials' dielectric properties through their dependence on the complex reflection coefficient and the propagation coefficient. Other issues of practical relevance are also addressed, namely, the fact that the dielectric properties of the waveguide filled with honey bee samples are essentially a mixture of two dielectric contributions, those from the bees and those for air pockets adjacent to the bees. The impact this has on measurements can be minimized through the use of a dielectric mixing model, which, in turn, provides an effective measure of the dielectric properties of interest. Several models exist for this purpose in the relevant literature [15]–[17]. For the purpose of this study, a two-component dielectric mixing model is used based on the Landau & Lifshitz and Looyenga relationships [18], [19]. The model assumes the form of the following equation:

$$\epsilon_{cm}^{1/3} = \nu_1 \cdot [\epsilon_{ca}]^{1/3} + \nu_2 \cdot [\epsilon_{cb}]^{1/3} \tag{1}$$

where ϵ_{cm} is the complex permittivity of the air–bee mixture, ϵ_{ca} is the complex permittivity of air pockets (or any other nonbee entity), and ϵ_{cb} is the average complex permittivity of the bees. The volumes ν_1 and ν_2 account for the fractional volumetric content for the nonbee and bee contents of the waveguide, respectively, and add up such that their total is 100% of the waveguide's total volumetric contents. The model (1) is, therefore, inverted in terms of ϵ_{cb} and solved for, where the fractional volumetric contents of the waveguide are determined through volumetric displacement, as shown in Fig. 1(b). The bee population used to fill the waveguide is submerged in a high-density acetone solution with total bee volume determined by volumetric displacement before and after the submerging of the bees with an absolute measurement precision of 0.1 ml. This together with the known volume of the waveguide and measured S-parameters completely determines quantities necessary for the computation of ϵ_{cb}.

C. Dielectric Characterization Results

Using the preceding formulation, the characterization of three different honey bee samples is undertaken. Measurement of dielectric properties for the different samples is to ensure the repeatability of observed results and to account for the variability of dielectric properties across different honey bee samples.

The measurement is undertaken across the X-band for a frequency range $\approx 8.2 \leq f \leq 12.4$ GHz with results summarized in Fig. 2. A high level of agreement across the three sample populations over the frequency range of interest is noted where, on average, the dielectric constant ϵ' undergoes an increase for the frequency range from 8.2 to 10 GHz, reaching a maximum at 10 GHz, but begins to undergo a monotonic decrease for a frequency beyond 10–12.4 GHz. The loss factor varies similarly across this frequency range with a tendency to undergo a limited decrease for frequencies from 8.2 to 9 GHz and undergoes a gradual increase beyond 9 GHz. On average, across this frequency range, the dielectric constant varies between 10.3 and 11.7, and the loss factor varies between 2.5 and 4.5. The limited variation noted, in particular with respect to the dielectric loss across the three sample

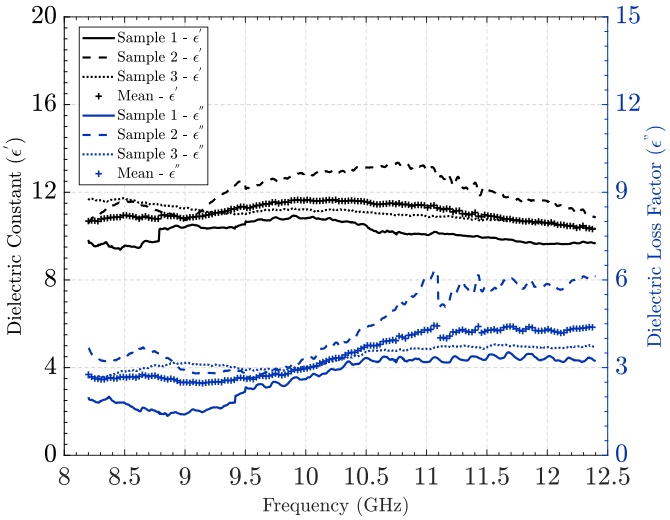

Fig. 2. Illustration of dielectric properties for three different honey bee samples. Depiction includes complex dielectric constant for the three honey bee samples separately and the final complex dielectric constant based on the average measurement(s) of the three populations.

populations, is attributed to natural variation in the dielectric properties of honey bees. Furthermore, measurement losses, absolute volume determination, and mixture inhomogeneities are all expected to have contributed to some of the observed variations. In what follows, these results are incorporated into numerical modeling simulations used to reliably model the honey bee RCS. The honey bee model used is predefined in SolidWorks [20], a computer-aided design (CAD), and computer-aided engineering (CAE) tool and later modified for the fidelity of the honey bee representation, as well as compatibility to Altair's FEKO.

III. Experimental Analysis and Validation

Further assessment of the relevant numerical modeling is undertaken through rigorous experimental analysis and measurement. This is done at the ElectroScience Laboratory, The Ohio State University, in the anechoic chamber [21]–[23] under the two principal polarizations horizontal (H-pol) and vertical (V-pol) at a range of frequencies of interest. An illustration of the experimental setup is shown in Fig. 3.

A. Practical Experimental Considerations

Prior to an empirical analysis of the honey bees' RCS, several issues of practical relevance are addressed. While reflections from the chamber's walls are minimized through the absorbers, reflections can never be completely eliminated. For this reason, the impact of artifacts introduced to the measurement due to these contributions is minimized through an initial series of tests aimed at quantifying the chamber's RCS signature over a wide range of frequencies and, subsequently, eliminating them through a background (clutter) subtraction from subsequent measurements. While this largely minimizes the impact of background reflections, their contribution is further minimized through the implementation of a time gating technique. In this, as part of the postprocessing procedure contributions at a series of time intervals t_1 to t_n is subjected to time gates aimed at eliminating returns known to have come from multipath effects or interactions of the target with the background environment, this goes to remove indirect paths in the compact range between the feed and the target. One of these paths is the direct leakage from the feed horn to the target, bypassing the reflector. Knowledge of exact target positions and locations of likely interferers is instrumental in this such that time gates are set about intervals known to be associated with these background reflections.

Other considerations relate to the contributions of the fixture used to hold the bee, namely, the styrofoam cup. In spite of the styrofoam cup's $\approx$ 2.1 dielectric constant [24] and its weakly scattering nature, it will have some impact on the measurement particularly taking into account the small physical extent of the honey bee samples and the sensitivity of the measurement to any perturbation in its orientation, rotational symmetry, time of measurement relative to the time of bee collection, frequency of operation, and polarization of the incident wave. For this reason, its RCS signature prior to the mounting of the honey bee is quantified across a wide range of frequencies and subsequently subtracted. Finally, absolute measurement calibration is undertaken on a band-by-band basis using objects whose RCS response is well understood. This includes spheres, cylinders, or plates composed of conducting material with spheres being the targets most commonly used in practice due to their pure azimuthal and rotational symmetry and, therefore, the invariance of its echo with orientation. Here, two conductive spheres with a diameter of 2.75 and 12 in were used, with results from both used for comparative analysis. For calibration standards verification, the RCS of both spheres was measured and compared to the Mie series theoretical (exact) solution [25] to ensure the convergence of both to the same frequency-dependent behavior. Using this setup, the measurement system is calibrated across the frequency range of interest.

B. Experimental Results

In order to validate numerical modeling results obtained using FEKO's MoM solver, several experimental measurements were conducted. Full measured azimuthal RCS profiles at three different frequencies compared against simulation results are depicted in Fig. 4 in which a high degree of correlation between the measured and modeled RCS signature is noted with a modest root-mean-square error (RMSE) across the depicted results. For Fig. 4(a), RMSE is 3.89 and 4.45 (dBsm), for Fig. 4(b), it is 3.25 and 7.57 (dBsm), and for Fig. 4(c), it is 5.07 and 3.95 (dBsm) for H-pol and V-pol, respectively. Furthermore, from Fig. 4 coupled with additional experimental analysis, it became evident that RCS is consistently higher for the bees' thorax and abdomen at $\varphi = \pm 90°$ and reaches a minima at $\varphi = 0°$ and 180°. This is to be expected due to the larger scattering surface of the abdomen and thorax relative to the smaller surface, which is associated with the scatterers at the latter set of azimuth angles. The larger RCS signature in terms of the magnitude of H-pol across the three different frequencies is noted with V-pol constantly attaining a lower magnitude regardless of frequency. This is to be expected as the bee's body length-to-height

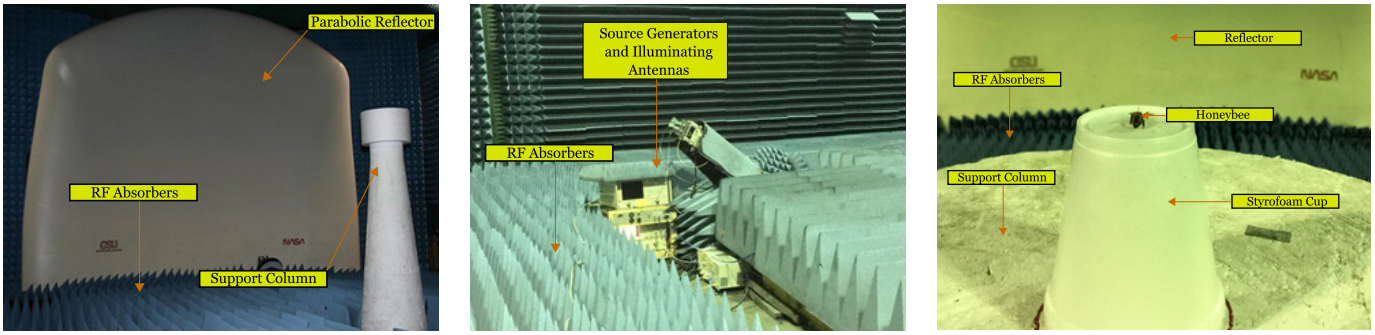

(a) (b) (c)

Fig. 3. Depiction of experimental setup at ElectroScience Laboratory compact range—anechoic chamber. (a) Reflector for achieving far-field test conditions. (b) Signal generators and illuminating antennas. (c) Target and its positioning on support beam.

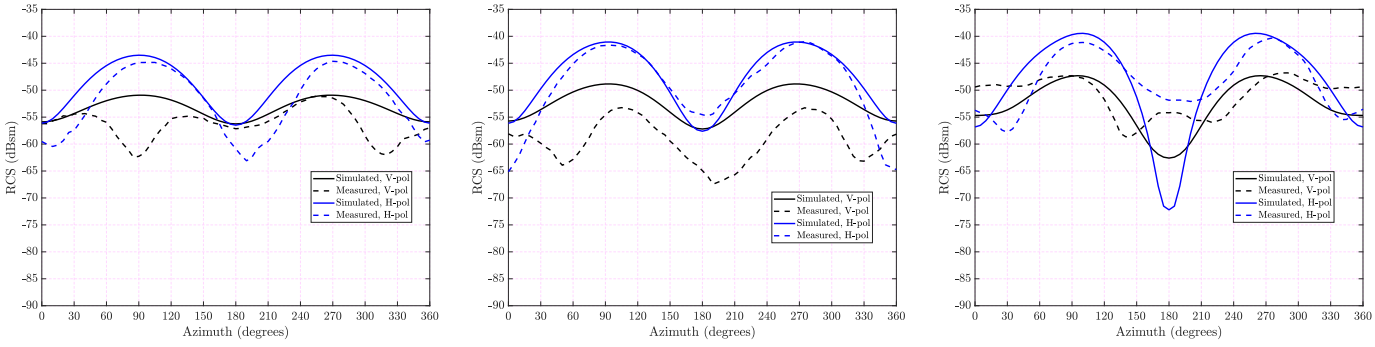

(a) (b) (c)

Fig. 4. Illustrations of honey bee RCS across different frequencies at the two principal polarizations, H-pol and V-pol, with comparisons of measured and simulated results. (a) Measurement and simulation comparisons at 8.5 GHz. (b) Measurement and simulation comparisons at 10 GHz. (c) Measurement and simulation comparisons at 12 GHz.

ratio is typically on the order of 4:1, while the diameter-to-height ratio is significantly less; therefore, V-pol illumination is backscattered due to reflection from a smaller interceptor (the bee's height) compared to H-pol (the bee's length).

IV. Discussion

While the results outlined in the preceding section are largely encouraging, illustrating clearly the capability of FEKO to capture intricacies in the bees' RCS as confirmed by experimental analysis, considerable effort is invested in investigating the sources of some of the observed experimental discrepancies. This includes the fact that consistently higher error levels are observed across all frequencies of interest for V-pol compared against H-pol measurements. This can be attributed to two main reasons, including the small physical diameter of the bee relative to its length, which makes all V-pol scatter susceptible to larger error levels. Furthermore, while the anechoic chamber's walls are covered with an identical distribution of absorbers the floor and ceilings are fitted with RF absorbers with a distribution that is not identical, an issue that is expected to have had an impact on V-pol scatter in particular.

In addition, higher error levels and distortions in the RCS patterns both from measured and simulated results are found to be associated with studies conducted at higher frequencies. This can be attributed to the reduction of wavelength size relative to the bees' size, thereby making it highly susceptible to perturbations brought about by structural variation in the actual bees' body and more prone to being affected by the interference caused by multipath and background contributions.

Furthermore, the bulk of honey bee samples used in this study were not killed and, instead, sedated with dry ice to temporarily immobilize them. For studies with increased time duration, the bees begin to move thereby introducing minor, but occasionally noticeable, discrepancies between measured and simulated RCS; this together with imperfections in honey bee sample placement played a role in increased error levels and the rotational symmetry of the azimuthal RCS profile. Other sources of error are related to the variation of the honey bees' dielectric constant over the observation period, in particular for studies that spanned more than 6 h or was conducted at higher latencies after bee collection in which the honey bee transitioned from wet to dry conditions. Moisture content, the bulk of which is within the honey bees' abdomen associated with end-on incidence $\varphi = 180°$, plays a major role in determining the overall dielectric constant for the sample, which, in turn, influences the observed RCS. An example of this effect is depicted in Fig. 5, where, for this particular sample, the measurement was taken directly after collection and 24 h after collection. Such variations in dielectric properties are expected to have introduced some error in

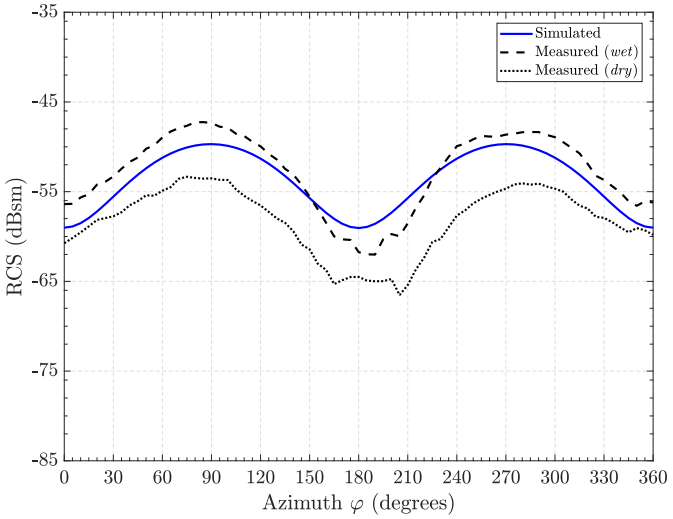

Fig. 5. Illustration of the impact measurement latency on empirical results relative to modeling results.

measurement in particular for studies conducted with higher latency where, in this case, it resulted in an increase in RMSE from 2.1 to 4.9 dBsm. Finally, while this study is concerned with RCS analysis over X-band, several experiments were also performed at higher frequencies. Similar overall tendencies were noted, with one main reason for the frequency range $13.2 < f \leq 14$ GHz is that a sharp and abrupt ≈30-dBsm decline is observed at end-on $\varphi = 180°$ incidence about the honey bees' abdomen. Taking into account that this is where the bulk of the bee's volumetric moisture content is contained, the rapid attenuation is attributed to the resonance of water within this frequency range [26].

While the aforementioned analysis attempts to provide insight into some of the reasons for observed discrepancies, the high degrees of correlation observed across experimental results relative to modeled results are, nonetheless, encouraging.

V. Conclusion

This letter provides a framework through which numerical analysis tools can be used to model the RCS of organisms of interest, which would potentially go to enable radar-based tracking of these creatures based on their modeled RCS signatures. This work specializes this framework for the case of the *Apis mellifera* honey bee and illustrates the potential of using FEKO's MoM solver for the purposes of modeling, reliably, the honey bee RCS under a wide range of frequencies for both H/V-pol. The results obtained from the relevant empirical analysis show a high degree of correlation with simulated RCS signatures with modest error levels, which, in turn, motivates the continued investigation and development of this approach.

While the bulk of the results are promising, several factors that increase the extent of error are discussed. Furthermore, the sensitivity of the measured RCS to variations in the bees' dielectric properties under dry/wet conditions is emphasized. Future efforts would, therefore, aim to further investigate these dependencies and the extent to which they will impact the outlined framework for radar-based detection and tracking applications.

References

[1] R. D. Judy *et al.*, *National Fisheries Survey*, vol. 1. Washington, DC, USA: U.S. Environmental Protection Agency, 1981.
[2] J. Ollerton, R. Winfree, and S. Tarrant, "How many flowering plants are pollinated by animals?" *Oikos*, vol. 120, no. 3, pp. 321–326, Mar. 2011.
[3] A.-M. Klein *et al.*, "Importance of pollinators in changing landscapes for world crops," *Proc. Roy. Soc. B, Biol. Sci.*, vol. 274, no. 1608, pp. 303–313, 2007.
[4] S. S. Chopra, B. R. Bakshi, and V. Khanna, "Economic dependence of U.S. industrial sectors on animal-mediated pollination service," *Environ. Sci. Technol.*, vol. 49, no. 24, pp. 14441–14451, 2015.
[5] K. Kulhanek *et al.*, "A national survey of managed honey bee 2015–2016 annual colony losses in the USA," *J. Apicultural Res.*, vol. 56, no. 4, pp. 328–340, 2017.
[6] D. B. Sponsler *et al.*, "Pesticides and pollinators: A socioecological synthesis," *Sci. Total Environ.*, vol. 662, pp. 1012–1027, Apr. 2019.
[7] S. S. Greenleaf, N. M. Williams, R. Winfree, and C. Kremen, "Bee foraging ranges and their relationship to body size," *Oecologia*, vol. 153, no. 3, pp. 589–596, Aug. 2007.
[8] M. Couvillon, R. Schürch, and F. Ratnieks, "Waggle dance distances as integrative indicators of seasonal foraging challenges," *PLoS ONE*, vol. 9, no. 4, 2014, Art. no. e93495.
[9] J. R. Riley, J. W. Chapman, D. R. Reynolds, and A. D. Smith, "Recent applications of radar to entomology," *Outlooks Pest Manage.*, vol. 18, no. 2, pp. 62–68, Apr. 2007.
[10] D. Mirkovic, P. M. Stepanian, C. E. Wainwright, D. R. Reynolds, and M. H. M. Menz, "Characterizing animal anatomy and internal composition for electromagnetic modelling in radar entomology," *Remote Sens. Ecol. Conservation*, vol. 5, no. 2, pp. 169–179, Jun. 2019.
[11] R. Wang *et al.*, "Migratory insect multifrequency radar cross sections for morphological parameter estimation," *IEEE Trans. Geosci. Remote Sens.*, vol. 57, no. 6, pp. 3450–3461, Jun. 2019.
[12] V. A. Drake, J. W. Chapman, K. S. Lim, D. R. Reynolds, J. R. Riley, and A. D. Smith, "Ventral-aspect radar cross sections and polarization patterns of insects at X band and their relation to size and form," *Int. J. Remote Sens.*, vol. 38, no. 18, pp. 5022–5044, Sep. 2017.
[13] *User's Manual*, FEKO Comprehensive Electromagn. Solutions,Johannesburg, South Africa, 2014. [Online]. Available: https://altairuniversity.com/uploads
[14] L. P. Ligthart, "A fast computational technique for accurate permittivity determination using transmission line methods," *IEEE Trans. Microw. Theory Techn.*, vol. MTT-31, no. 3, pp. 249–254, Mar. 1983.
[15] G. Banhegyi, "Comparison of electrical mixture rules for composites," *Colloid Polym. Sci.*, vol. 264, no. 12, pp. 1030–1050, Dec. 1986.
[16] A. H. Sihvola, *Electromagnetic Mixing Formulas and Applications*, no. 47. London, U.K.: IET, 1999.
[17] S. O. Nelson, "Useful relationships between dielectric properties and bulk densities of granular and powdered materials," in *Proc. Amer. Inst. Chem. Eng. Annu. Meeting*, 2004, pp. 136–140.
[18] D. C. Dube, "Study of Landau-Lifshitz-Looyenga's formula for dielectric correlation between powder and bulk," *J. Phys. D, Appl. Phys.*, vol. 3, no. 11, pp. 1648–1652, Nov. 1970.
[19] S. O. Nelson, "RF and microwave permittivities of insects and some applications," in *Proc. URSI EMTS Int. Symp. Electromagn. Theory*, 2004, pp. 1224–1226.
[20] *SolidWorks*, Dassault Syst., Vélizy-Villacoublay, France, 2015.
[21] T.-H. Lee and W. D. Burnside, "Performance trade-off between serrated edge and blended rolled edge compact range reflectors," *IEEE Trans. Antennas Propag.*, vol. 44, no. 1, pp. 87–96, Jan. 1996.
[22] T.-H. Lee and W. D. Burnside, "Compact range reflector edge treatment impact on antenna and scattering measurements," *IEEE Trans. Antennas Propag.*, vol. 45, no. 1, pp. 57–65, Jan. 1997.
[23] E. Walton and J. Young, "The Ohio State University compact radar cross-section measurement range," *IEEE Trans. Antennas Propag.*, vol. AP-32, no. 11, pp. 1218–1223, Nov. 1984.
[24] E. Knott, *Radar Cross Section*. Boston, MA, USA: Artech House, 1993.
[25] M. Skolnik, *Introduction to Radar Systems*. New York, NY, USA: McGraw-Hill, 1980.
[26] C. Levis, J. T. Johnson, and F. L. Teixeira, *Radiowave Propagation: Physics and Applications*. Hoboken, NJ, USA: Wiley, 2010.